

Proceedings of the Korean Nuclear Society Autumn Meeting  
Taejon, Korea, October 2000

## **Flow Structure and Near-Wall Bubble Behavior in Subcooled Flow Boiling at High Heat Flux**

**In Cheol Bang, Won-Pil Baek and Soon Heung Chang**

Department of Nuclear Engineering  
Korea Advanced Institute of Science and Technology  
373-1, Kusong-dong, Yusong-gu, Taejon, 305-701, Korea

### **ABSTRACT**

The behavior of near-wall bubbles in subcooled flow boiling has been investigated photographically to identify the physical mechanisms of the boiling and the Critical Heat Flux(CHF) at subcooled and low-quality conditions. Visualization experiments were performed for water flow in vertical rectangular channels with one-side heating at mass flux of 1500 kg/m<sup>2</sup>s under atmospheric pressure. The bubble coalescence phenomena and a flow structure of the near-wall bubble layer were examined with the aids of a professional digital camera. The number of activated nucleation sites and coalescent bubbles increased somewhat linearly as the wall heat flux was increased. The increased number of near-wall bubbles and the appearance of some crowded areas occupied by large bubbles resulting in a vapor clot were observed when the heat flux was further increased. At sufficiently high heat flux (60-70 %CHF), the appearance of the vapor clot or blanket on the heated surface began to play a role of an obstacle between main liquid region and the region near heated wall.

At such high heat flux, three characteristic regions were observed in the heated channel: (a) a superheated liquid layer with attached bubbles on the heated wall, (b) a flowing bubble layer consisting of large coalesced bubbles over the superheated liquid layer, and finally (c) the liquid core over the flowing bubble layer.

In this flow structure, the CHF seems to occur at an instant of the process of periodic formation of large vapor clot near the channel exit. According to the visualization, the CHF mechanism is related to the formation of the large vapor clots resulting from coalescences of bubbles and the evaporation of the liquid layer under those clots.

### **1. INTRODUCTION**

Forced convective nucleate boiling is very effective in achieving high a heat flux with a small temperature difference between the heated surface and the cooling fluid; however, there is a boundary of this effective heat transfer regime, called the departure from nucleate boiling (DNB). Understanding of this DNB phenomenon is important for effective and safe operations of nuclear systems and other thermal-hydraulic areas.

However, the mechanism leading to DNB has not been clearly understood yet. This is

mainly due to the fact that detailed observation of the near-wall region at high heat and mass fluxes is very difficult. Some experimenters such as Gunther(1951), Jiji & Clark(1962), Tong et al.(1966), Celata et al.(1995) and Galloway & Mudawar(1993) have tried to get rid of this difficulty by means of various flow visualization tests. Their works have focused mainly on bubble parameters within the bubble boundary layer and bubble behaviors related on the occurrence of DNB. Gunther(1951) investigated bubble-growth-collapse process and measured maximum bubble size, bubble growth and collapse rates, bubble population, and fraction of the surface covered by bubbles. The study showed that an increase of heat transfer rate causes bubble population to increase up to a limit where bubbles coalesce to vapor clumps and bubble coalescence signifies incipient film boiling and burnout. Bibeau and Salcudean(1994) performed the boiling experiments using a vertical circular annulus at 1 atm, for mean water flow velocities of 0.08-1.2 m/s and subcoolings of 10-60°C. The study showed that bubbles did not grow and collapse on the heated wall, but ejected into the flow for subcoolings below 60°C and after the onset of nucleate boiling, bubbles slide away from the nucleation site and later ejected into the flow. Zeitoun and Shoukri(1996) using water and a vertical concentric annular test section found that the bubble departure was not the reason for the net vapor generation(NVG) phenomenon and the increase in bubble size due to decrease in condensation and bubble coalescence was the main reason for the significant increase in void fraction along the heated channel.

Jiji and Clark(1962) investigated the bubble boundary layer and correlated its thickness for water and a rectangular channel. The study showed that the bubble boundary layer thickness increased with increasing distance from the leading edge by an increase in bubble size and a thin layer of superheated vapor is formed over the heated surface as the maximum heat flux is approached. Tong et al.(1966) identified the effect of mass flow rate on bubble size and correlated the bubble size for freon-113 rectangular channel. In particular, they suggested the existence of a superheated liquid layer on the heated wall. Their results showed that the bubble-diameter size at or near departure from a vertically heated surface was inversely proportional to mass velocity to the 1/3 power during subcooled nucleate boiling flow. Del Valle and Kenning(1985) found that the startup of new sites deactivated many of the sites active at lower wall superheat and the flow regime changed from bubbly flow regime to slug flow one in decrease of subcooling for water rectangular channel. They reported data for active nucleation site density showed a linearity as a function of heat flux.

Mattson et al.(1973) also correlated the bubble size and the bubble boundary layer thickness, and found that the vapor phase attained a higher velocity than the liquid phase for freon-113 rectangular channel. The study showed the bubbles moved along the heater before departure, the bubble size on the heater was largest at the DNB, and the vapor velocity was low on the heater at the DNB. Thus, they reported that as the DNB was approached the bubbles on the heater began to pile up on one another(agglomerate) towards the downstream end of the heater. Celata et al(1995) observed that the vapor blanket was rooted to the nucleation site on the heated surface in high subcooling condition about 164K for water annulus channel.

Various mechanisms have been reported as the causes of DNB but no theoretical models with good prediction performance are tightly linked to such reported experimental results.

Digital photographic technique has significantly advanced for recent decades. This

would enable researchers to overcome some difficulties of visualization study in relation to complex boiling phenomena.

In this study, by using digital photographic techniques, not only some boiling characteristics such as distribution of bubble size, nucleation site density and bubble boundary layer thickness but also bubble coalescence and flow structure were examined for the subcooled flow boiling of water in a rectangular channel with one-side heating.

## 2. EXPERIMENTS

### 2.1 Experimental apparatus

Subcooled flow boiling tests have been performed with water at atmospheric pressure, for mass flux of  $1500 \text{ kg/m}^2\text{s}$  and inlet subcooling of  $53^\circ\text{C}$ . Figure 1 shows the schematic of the experimental loop which consists of the following components: a centrifugal pump, a turbine flow-meter, two pre-heaters, a test section, a condenser, a surge tank and a liquid reservoir. Electrical power was supplied as the direct current by means of a rectifier with the maximum power of 64 kW (32 V and 2000 A).

Three test sections have been manufactured and used up to now. Step by step, they have been modified to achieve more light amount in the visual area. Their basic structure and characteristics are shown in Fig. 2. The test section is a rectangular type which is vertically oriented. It consists of two components: a channel body and an inserter containing a heating plate. The body is made of aluminum alloy and provides a flow channel of  $8 \text{ mm} \times 5 \text{ mm}$ , and Lexan windows for visualization at front and side parts. The inserter is made of Bakelite as an insulator and a stainless steel heating plate with the size of  $4 \text{ mm}$  (width)  $\times$   $100 \text{ mm}$  (length)  $\times$   $2 \text{ mm}$  (thickness). The plate is heated by the DC current supplied by copper electrodes connected at both ends. The Bakelite insulator assures a sufficient insulation to allow only a negligible heat loss to surrounding air.

### 2.2 Photographic Techniques

The visualization of the flow channel was achieved by the aid of an 8 mm-camera recorder, a still camera and a high-speed camera from the left side and the front. A

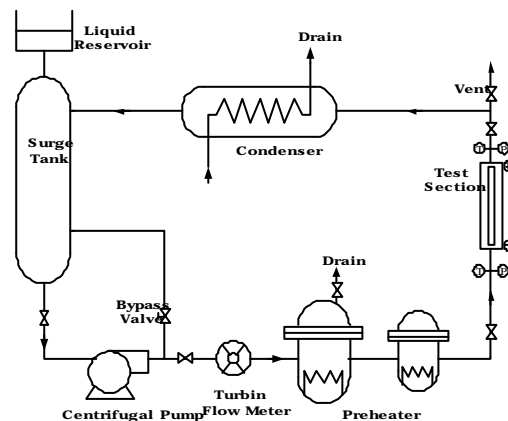
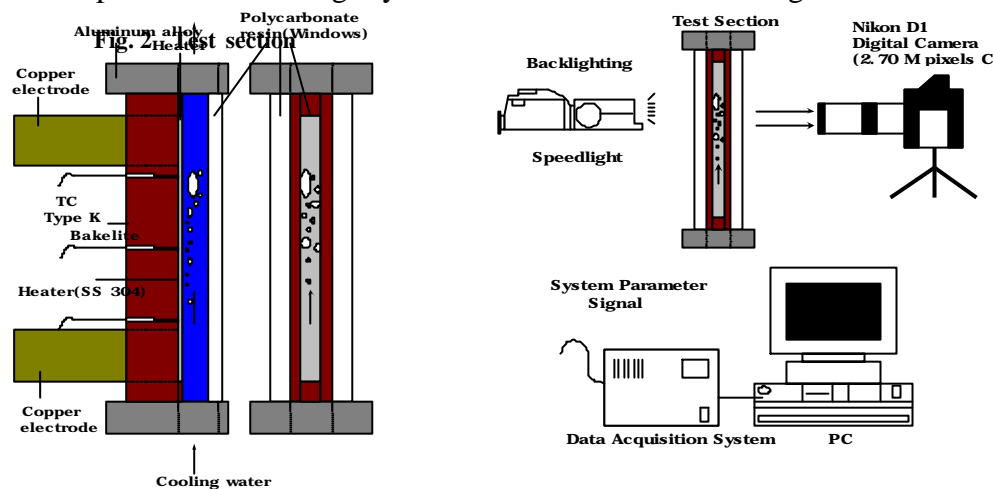


Fig. 1. Schematic diagram of test loop

Kodak Ektapro 1000 motion analyzer as a high speed camera was used at speeds of 500 and 1000 frames per second but clear images could not be acquired due to poor resolution and low speed. Still photographs were taken originally with a Nikon FM2 camera. A Nikon D1 digital camera with 2.74 million pixels, 1/500 second of flash-synchronized speed was finally used considering the advanced image resolution and speed.

Photographic technique of using only the flash speed was adopted for acquiring the clear stop image of fast bubbles and disturbing boiling states. While the shutter was open, a high-speed flash of 1/8700 second was emitted to the flow channel with backlighting in case of lateral observation. The light source was a Nikon Speedlight SB-28 model. Figure 3 shows the photographic system with the data acquisition device.

Nikon 105 mm Micro lens and the three extension tubes of 14 mm, 21 mm and 31 mm for the close-up were used to magnify the flow channel. The focusing of the camera was



**Fig. 3 Photographic system and DAS**

fixed on the heating surface at front observation and near the middle point of the flow width at side observation. Three Halogen lamps as the light source were set near visual windows. Two of those are of 300 W power and the other is of 500 W power. After a capture of a bubble motion, the image processing was performed mainly on the brightness and contrast of an image. Continuous photos were taken at the time interval of 0.22 second. Front observation and lateral observation were performed separately. The visualization study in this work has so far been focused not on a single bubble but on overall behavior of the bubble layer because the overall phenomena of flow structure is important from the viewpoint of flow boiling

### 3. RESULTS AND DISCUSSION

The visualization of near-wall regions has made an identification of the flow structure, the size of which is about several tens of microns. After front observation of nucleate boiling to DNB, lateral observation was made. Fig. 4 shows the change of the activated nucleation site density on the heated surface according to the changes of the heat flux. The activation of nucleation sites is in proportion to the heat flux and the heating distance. Maximum bubble diameter also has the same trend. A correlation for the

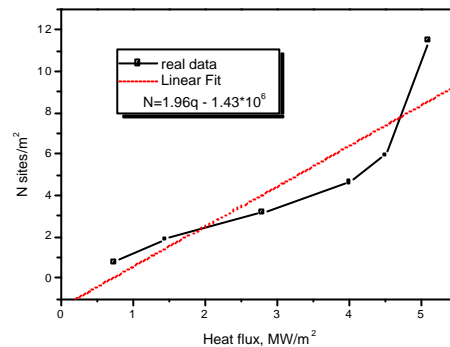


**Fig. 4 Nucleation site density versus heat flux**

nucleation site density was acquired through linear fitting. The result has a similar trend with Del Valle and Kenning(1985)'s. Nucleation site density has the order of million per square meter in flow boiling.

Figures 5 and 6 show nucleate boiling phenomena according to increasing heat flux, which were observed through front and lateral windows. At low heat flux, small bubbles with the size of a few micron, grow and move along heating surface. These bubbles form a big bubble with the size of 2-3 bubbles. As heat flux increases, adjacent nucleation sites become active and bubbles grow closely. Then adjacent bubbles merge each other or to big bubbles over the heating surface. At high heat flux near 80% CHF, vigorous coalescing of neighboring bubbles is observed. In that point, bubbles seem to cover most of the heating surface. More nucleation sites and larger vapor clots are observed for the higher heat flux level and for the higher channel-averaged quality.

Figures 7 and 8 show overall visual results on the effects of both heated length and heat flux on bubble behavior. Bubbles near the heated surface are coalesced with each other and become a big vapor clot or blanket. The merging of growing bubbles and flowing bubbles departed from the heated surface would be the cause of formation of these vapor clots. Sometimes, while these large bubbles neighboring themselves grow, they are merged with each other and covered over the half of surface in width direction. After the merging of large bubbles, a vapor clot departed the heated surface. The area fraction of vapors covering the heated surface occasionally had the values over 50 % in 10 mm of the heater end part.

As the heat flux increases, the area fraction of vapor for heated surface proportionally increases and the distance between them decreases. At higher heat flux, some vapor clot seemed to burst and spread around the center of it. Though the photographs were taken at the same conditions of mass flux, heat flux and subcooling, the acquired photographs had different characteristics in case that the direction of putting the light from flash changed. For example, backlighting and front lighting give clear images for near-wall bubbles while lateral lighting gives clear images of flowing bubbles. The overlapping of flowing bubbles and vapor clots over the heated surface gives the disorder to the spatial depth. The outer surface of vapor blankets or clots looks to drag into the direction of the outlet of test section by means of the effect of faster liquid phase. At sufficiently high heat flux about 75% CHF, the appearance of vapor clots or blanket on the heated surface made a role of an obstacle between main liquid region and the region near heater. These vapor clots due to coalescing of bubbles appear with a time interval which is related to bubble frequency. And also these sometimes form a larger vapor clot and it looks like a

wave as shown in Fig. 9. Fig. 8 also shows bubble boundary layer thickness and near-wall bubble layer grow together from the leading edge to the exit.

Figures 9 and 10 show the near-wall phenomena on the overall heated surface near the DNB condition. Continuous photos with time interval of 0.22 second show that large vapor clot has a form of wave and a period of formation and disappearance. In particular, large vapor clots of Fig. 10 have many wall-attached bubbles beneath and around themselves, indicating that the formation mechanism might be due to the fast merging of neighboring bubbles. The appearance of vapor clot larger than other some clots in other time is related to not only fast merging of adjacent bubbles but also additional coalescence of flowing detached bubbles. Most of coalesced vapor is observed over 70% heating length. As the DNB condition is approached, small bubbles are observed inside large vapor blanket. This means that coalescence between consecutive bubbles near the wall and some layer with bubbles below vapor blanket exists. Vapor clots have average size of 10 mm long and 2-3 mm diameters. At a high heat flux, it is also observed that vapor film formed locally on heated wall exists between wall bubbles and liquid. Fig 11 shows magnifying vapor film on heated wall.

In this experiment, DNB occurred at  $6.4 \text{ MW/m}^2$ . Figure 12 shows continuous phenomena at and after DNB occurrence. The region occupied by large vapor clots moved downward and upward because of low heat transfer due to vapor film formed on DNB occurrence location. Heated surface were severely damaged by a sudden temperature rise.

Present observations indicate a flow structure of three layers:

- the superheated liquid layer with very small bubbles attached on the heated surface
- the flowing bubble layer containing vapor clots and small bubbles (coalescence occurs in this layer.)
- the liquid core over the flowing bubble layer.

#### 4. CONCLUSIONS

The behavior of near-wall bubbles in subcooled flow boiling has been photographically investigated for water flow under atmospheric pressure. The main observations are as follows:

(a) The number of activated nucleation sites increases with the increase in the surface heat flux and with the decrease in channel-averaged local subcooling;

(b) At sufficiently high heat flux about 70 % CHF, the appearance of the vapor clot or blanket on the heated surface acts as an obstacle for liquid flow from the main liquid core region to the superheated liquid layer near the heater;

(c) At sufficiently high heat flux, three characteristic regions were observed in the heated channel: (i) a superheated liquid layer with attached bubbles, (ii) a flowing bubble layer consisting of large coalesced bubbles, and (iii) the liquid core; and

(d) The CHF occurred during the process of periodic formation of largely vapor clots near exit.

Further investigation would be required for more reliable identification of DNB mechanisms according to various flow conditions.

## 5. REFERENCES

- Bibeau, E.L and Salcudean (1994), A study of bubble ebullition in forced convective subcooled nucleate boiling at low pressure, *Int. J. Heat Mass Transfer*, Vol. 37, 2245-2259
- Celata, G.P., Cumo, M., Mariani, A. and Zummo, G. (1995). "Preliminary remarks on visualization of high heat flux burnout in subcooled water flow boiling", *Two-phase flow modeling and experimentation*, 859-866
- Chun, T.H., Baek, W.P. and Chang, S.H. (2000). "An Integral Equation Model for Critical Heat Flux at Subcooled and Low Quality Flow Boiling", *Nucl. Eng. Des.*, Accepted for publication in 1999
- Del Valle, Victor H. and Kenning, D.B.R. (1985). "Subcooled flow boiling at high heat flux", *Int. J. Heat Mass Transfer*, Vol. 28, No 10, 1907-1920
- Fiori, M.P. and Bergles, A.E., (1970). "Model of critical heat flux in subcooled flow boiling", *Proc. 4<sup>th</sup> Int. Heat Transfer Conf., Versailles, France, Vol. IV*, p.B6.3.
- Galloway, J.E. and Mudawar, I. (1993). "CHF mechanism in flow boiling from a short heated wall - I, Examination of near-wall conditions with the aid of photomicrography and high-speed video imaging", *Int. J. Heat Mass Transfer*, Vol. 36, 2527-2540
- Gunther, F.C. (1951). "Photographic study of surface-boiling heat transfer to water with forced convection", *Trans. ASME*, Vol. 73, 115-121
- Ha, S.J. and No, H.C., (2000). "A dry-spot model of critical heat flux applicable to both pool boiling and subcooled forced convection boiling", *Int. J. Heat Mass Transfer*, 43, 241-250
- Jiji, L.M. and Clark, J.A. (1962). "Bubble boundary layer and temperature profiles for forced convection boiling in channel flow", *Trans. ASME, J. heat transfer*, 50-58
- Kirby, G.J., Stainforth, R. and Kinneir, J.H., (1967). "A visual study of forced convection boiling – Part 2. Flow patterns and burnout for a round test section", *AEEW-R-506, UKAEA, Winfrith*
- Kureta, M. and Akimoto, H., (1998). "Experimental study on critical heat flux along one-side heated rectangular channel under subcooled conditions", *6<sup>th</sup> ICONE-6226*
- Mattson, R.J., Hammitt, F.G. and Tong, L.S. (1973). "A photographic study of subcooled flow boiling and the boiling crisis in Freon-113", *ASME paper*, 73-HT-39
- Nariai, H., Kinoshita, H., Yoshida, T. and Inasaka, F., (1997). "Effect of tube length on the CHF of subcooled flow boiling", *2<sup>nd</sup> Japanese-German Symposium on Multi-Phase Flow, Tokyo*

Sturgis, J.C and Mudawar, I., (1999). "Critical heat flux in a long, rectangular channel subjected to one-sided heating-I. Flow visualization", *Int. J. Heat Mass Transfer* 42, 1835-1847

Tong, L.S., Bishop, A.A. and Efferding, L.E. (1966). "A photographic study of subcooled boiling flow and DNB of Freon-113 in a vertical channel", ASME paper, 66-WA/HT-3

Zeitoun, O. and Shoukr, M.,(1996) Bubble behavior and mean diameter in subcooled flow boiling, *Trans. ASME*, Vol. 118, 110-116

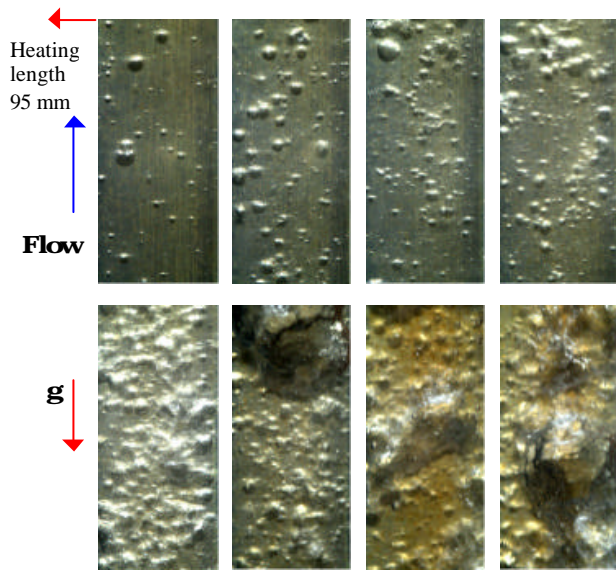


**Fig. 5 Effect of heat flux on bubble behavior**

Area 4\*10, Inlet Temp. 53° C, Pressure 1 atm  
 1.45(22.7%), 2.8(43.8%), 4.0(62.5%), 4.5(70.3%) MW/m<sup>2</sup>,  
 (quality (-x))=0.01431, 0.01053, 0.00716, 0.00576)  
 5.1(79.7 % CHF), 5.8(90.6%), 6.0(93.7%), 6.3(98.4%) MW/m<sup>2</sup>  
 (quality (-x))=0.00407, 0.00211, 0.00155, 0.00071)

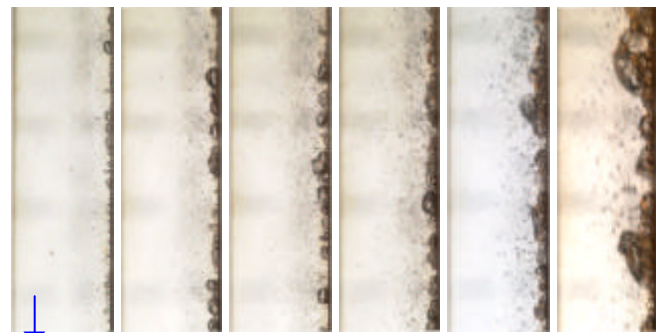


**Fig. 6 Effect of heat flux on bubble behavior**

Area 5\*18, Inlet Temp. 53° C, Pressure 1 atm  
 2.0(31% CHF), 3.2(50%), 4.0(63%),  
 5.0(78%), 5.6(88%), 5.9(92%) MW/m<sup>2</sup>,  
 (quality (-x))=0.01277, 0.0094, 0.00716, 0.00435, 0.00267, 0.00183)

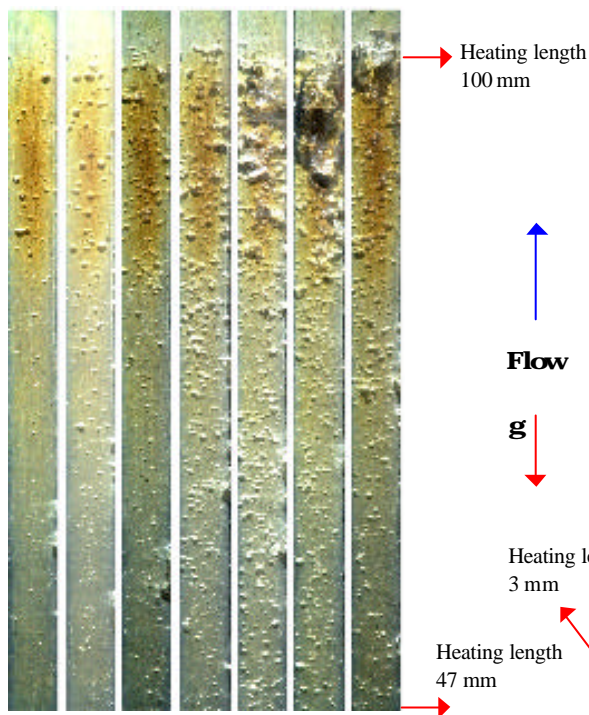


**Fig. 7 Effect of heating length on bubble behavior**

Area 4\*60, Inlet Temp. 53° C, Pressure 1atm  
 (%CHF)1.8(28.1%)2.4(37.5%)3.2(50%)4.0(62.5%)  
 4.8(75%) 5.3(82.8%)6.2(96.9%) MW/m<sup>2</sup>  
 (quality (-x))=0.01333, 0.01165, 0.00940,  
 0.00716, 0.00492, 0.00351, 0.00099)

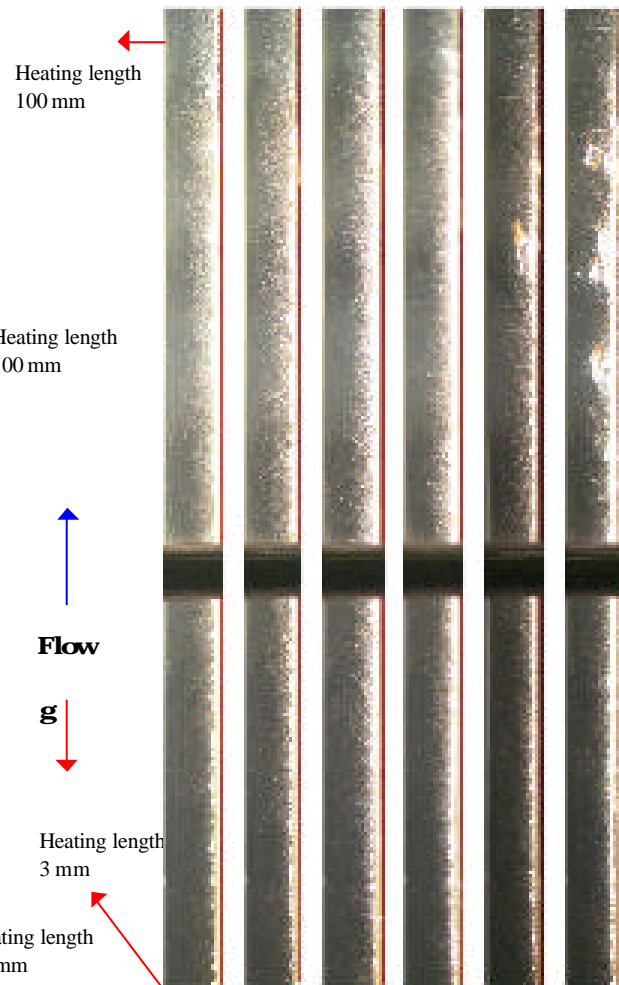


**Fig. 8 Bubble behavior along the heating length and heat flux**

Area 5\*102, Inlet Temp. 53° C, Pressure 1 atm  
 2.5(39%), 3.2(50%), 4.1(64%), 5.2(81%), 5.6(88%), 6.0(94%) MW/m<sup>2</sup>,  
 (quality (-x))=0.01137, 0.0094, 0.00688, 0.00379, 0.00267, 0.00155)

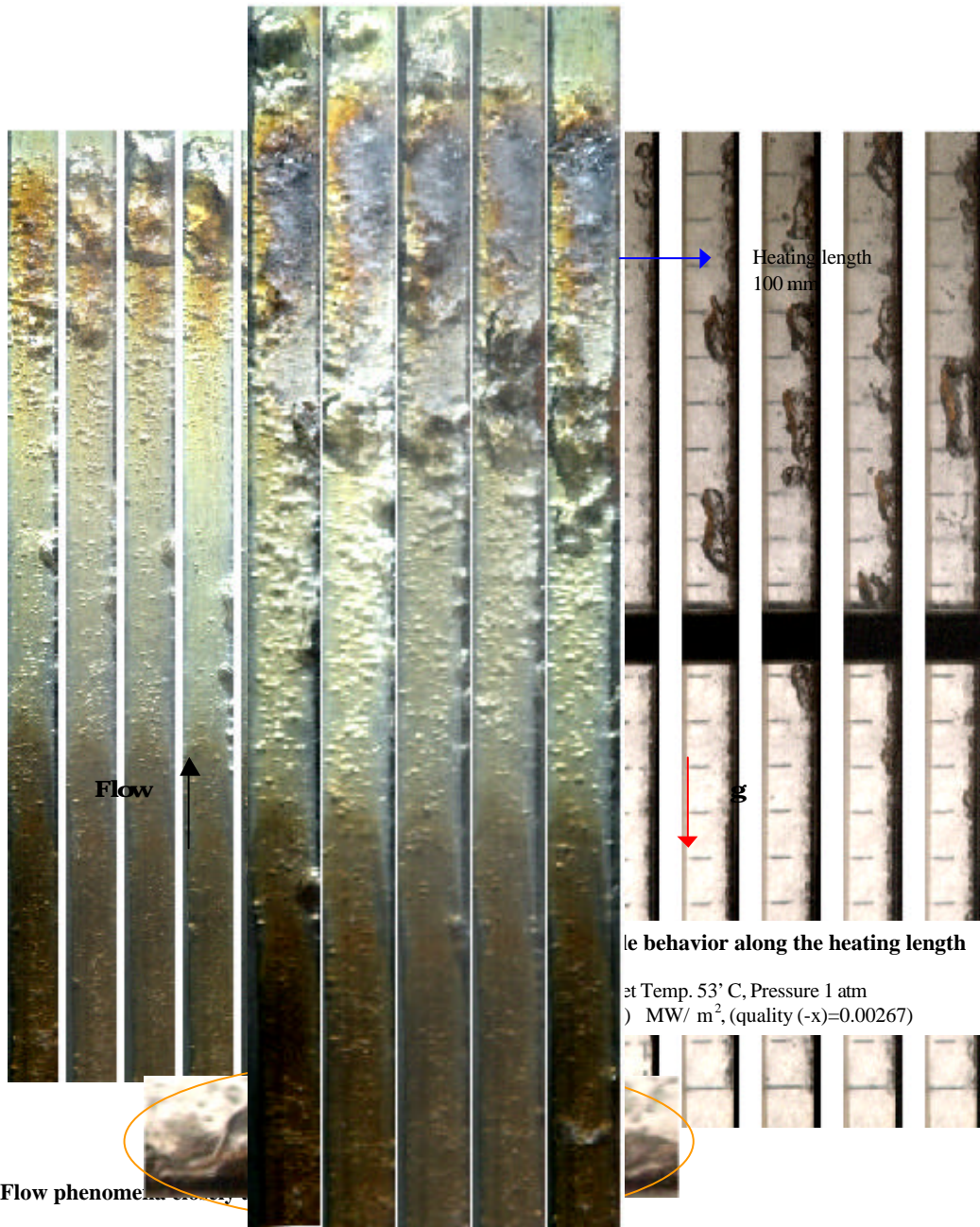


**Fig. 9 Flow phenomena**

Inlet Temp. 53 °C, Pressure 1atm (-x=0.00071, 0.000428)  
 6.3(98.4)6.3(98.4)6.3(98.4)6.3(98.4)6.3(98.4)6.3(98.4) MW/m<sup>2</sup>

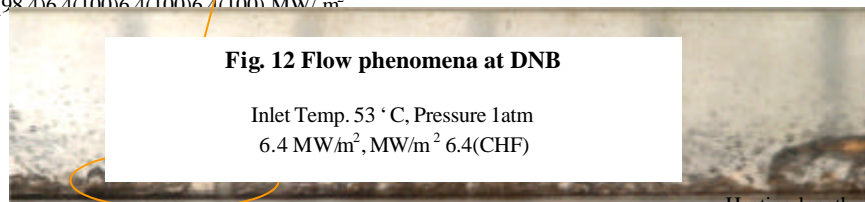


**Fig. 11 Vapor film on heated wall at 5.6(88%) MW/ m<sup>2</sup>**  
 Inlet Temp. 53 °C, Pressure 1 atm( quality (-x)=0.00267)